

Study on Fluid-Solid-Heat Coupled Numerical Simulation of Bathroom Wind-Warm

Jiajia Yu^{*1}, Yi Long²

¹Department of Electronic and Computer Engineering, Southeast University Chengxian College, Jiangsu, Nanjing, 210088, China

²School of Energy and Mechanical Engineering, Nanjing Normal University, Jiangsu, Nanjing, 210023, China

Keywords: numerical simulation, wind heating, thermal comfort

Abstract: A good air quality environment in the bathroom will bring a more comfortable showering experience. In winter, people use wind heating to heat the air in the bathroom to increase the ambient temperature during showering. The installation position of wind heating in a bathroom has a significant impact on the airflow organization and movement as well as human thermal comfort in the bathroom. In this paper, the method of numerical simulation is used to study the heat transfer process of a brand of bathroom wind heaters. The structure of the bathroom and the human skin tissue are simplified. The velocity and temperature fields of the air and human body models in the bathroom are obtained for different installation positions (overhead and side) and different heating powers (2,200w, 2,000w, 1,800w and 1,600w respectively) of the wind heating. The comparison focused on the effect of different installation positions on the human body during showering at the same heating power. By comparison, it was found that inlet 1 as the air inlet was 100cm away from the human shower position, which did not bring obvious wind sensation and its heat transfer effect could meet the thermal comfort of human body in the shower.

1. Introduction

Radiant bathroom heaters are cheap, common in the market, and it is a class of bathroom shower heating equipment has been widely used. However, the heat of traditional radiant bathroom heaters is concentrated in the local skin of the human body, which may burn the human skin due to high temperature for a long time, and if the bathroom heaters are in a humid environment for a long time, it may cause safety accidents[1]. Second, the blue light from radiant bathroom heaters can penetrate the lens and reach the retina, which can cause optical damage and accelerate the oxidation of macular cells. Especially for families with infants and toddlers, babies are too young to avoid the bright light of bathroom heaters, which may cause macular burns. Although adults do not stare at bathroom heaters, the light intensity of bathroom heaters can also affect the visual experience after bathing. Based on the above background, a new type of wind heating heater was created in the market[2]. The basic principle is that cold air enters from one end of wind heating and becomes hot air through the agitation of fan and heating by PTC ceramic heating element inside and then enters the bathroom from the air outlet. Then, the hot air circulates in the bathroom and heats up the room air to make the room temperature rise.

2. Methods

2.1 Governing Equations

Turbulence is very common in nature. Compared to other laminar motions in nature, turbulence has more distinctive features, i.e. it has many physical and mathematical nonlinear properties[3]. It is difficult to understand and explain turbulence clearly from theoretical analysis and experimental research. Therefore, with the gradual development of computer technology, numerical models can be used to understand turbulent motion. Both the analysis and calculation of hydrodynamics must

satisfy the laws of fluid motion, i.e. the law of conservation of mass, the law of conservation of momentum and the law of conservation of energy[4]. From the previous conclusions, it is assumed that air is incompressible in the bathroom. In the case of viscous air flow, relevant equations are mainly as follows:

1) Law of conservation of mass

The mass of a defined fluid is not born or destroyed during the motion. Any flow problem must satisfy the law of conservation of mass. This law can be expressed as the increase in mass per unit time in a fluid micro-element, equal to the net mass flowing into the micro-element in the same time interval. This equation is applicable to both the flow process of compressible fluids and the flow process of incompressible fluids.

The conservation of mass equation is:

$$\frac{\partial \rho}{\partial t} + \frac{\partial(\rho u)}{\partial x} + \frac{\partial(\rho v)}{\partial y} + \frac{\partial(\rho w)}{\partial z} = 0 \quad (1)$$

ρ denotes the fluid density; t denotes the time of fluid motion; u , v , and w represent the fractional velocities of the fluid in different vector directions of x , y , and z , respectively;

Since the fluid in this study is incompressible, ρ is zero, and the above equation changes to:

$$\frac{\partial u}{\partial x} + \frac{\partial v}{\partial y} + \frac{\partial w}{\partial z} = 0 \quad (2)$$

The conservation of mass equation is also often referred to as the continuity equation in the motion of fluids.

2) Momentum conservation equation

$$\frac{\partial u_x}{\partial t} + u_x \frac{\partial u_x}{\partial x} + u_y \frac{\partial u_x}{\partial y} + u_z \frac{\partial u_x}{\partial z} = -\frac{1}{\rho} \frac{\partial p}{\partial x} + f_x + \nu \nabla^2 u_x \quad (3)$$

$$\frac{\partial u_y}{\partial t} + u_x \frac{\partial u_y}{\partial x} + u_y \frac{\partial u_y}{\partial y} + u_z \frac{\partial u_y}{\partial z} = -\frac{1}{\rho} \frac{\partial p}{\partial y} + f_y + \nu \nabla^2 u_y \quad (4)$$

$$\frac{\partial u_z}{\partial t} + u_x \frac{\partial u_z}{\partial x} + u_y \frac{\partial u_z}{\partial y} + u_z \frac{\partial u_z}{\partial z} = -\frac{1}{\rho} \frac{\partial p}{\partial z} + f_z + \nu \nabla^2 u_z \quad (5)$$

Fluid dynamic system must also meet the law of conservation of momentum. The law of conservation of momentum can be expressed as the change rate of the momentum of a micro element with respect to time equal to the sum of all external forces acting on the micro element. This law actually reflects the second law of Newton. For an incompressible Newtonian fluid, the conservation of momentum equation in x , y and z directions can be derived from Newton's second law, which is referred to as the N-S equation .

where, ρ denotes the air density; ν denotes the coefficient of motion viscosity; u_x , u_y , u_z denotes the velocity vector of air in x , y , and z directions; f denotes the mass force per unit mass.

The left part of this equation represents the acceleration of the fluid microcluster in each direction, and the right part is the positive pressure, bulk force, and viscous shear force on the fluid microcluster. The N-S equation accurately describes the actual flow, and the analysis of the flow of viscous fluids can be reduced to the study of this equation.

3) Energy conservation equation

$$\frac{\partial}{\partial t}(\rho E) + \nabla \cdot (\bar{v}(\rho E + p)) = \nabla \cdot \left(k_{\text{eff}} \nabla T - \left(\sum_j h_j \bar{J}_j + (\bar{\tau}_{\text{eff}} \cdot \bar{v}) \right) \right) + S_h \quad (6)$$

$$E = h - \frac{p}{\rho} + \frac{v^2}{2} \quad (7)$$

The law of conservation of energy is also one of the several fundamental laws that must be satisfied throughout the motion of a fluid. The law of conservation of energy is essentially the first theorem of thermodynamics. The equation of conservation of energy can be written in the following

form:

where, K_{eff} is the effective thermal conductivity, and K_t in $K+K_t$ is the turbulent thermal conductivity defined according to the turbulence model used. J_j is the diffusive flux of fluid j . The first three terms on the right-hand side of Equation (6) represent the energy transfer due to conduction, continuous medium diffusion and viscous dissipation, respectively. The symbol S_h denotes the defined volumetric heat source. In Equation (6), E is expressed as follows:

$$E = h - \frac{P}{\rho} + \frac{v^2}{2} \quad (7)$$

4) The modeled transport equations for K and ε in the RNG $K-\omega$ model are:

$$\frac{\partial(\rho k)}{\partial t} + \frac{\partial(\rho k u_j)}{\partial x_j} = \frac{\partial}{\partial x_j} \left[\left(\mu + \frac{\mu_t}{\sigma_k} \right) \frac{\partial k}{\partial x_j} \right] + G_k + G_b - \rho \varepsilon - Y_M + S_k \quad (8)$$

and

$$\frac{\partial(\rho \varepsilon)}{\partial t} + \frac{\partial(\rho \varepsilon u_j)}{\partial x_j} = \frac{\partial}{\partial x_j} \left[\left(\mu + \frac{\mu_t}{\sigma_\varepsilon} \right) \frac{\partial \varepsilon}{\partial x_j} \right] + \rho C_1 S_\varepsilon - \rho C_2 \frac{\varepsilon^2}{k + \sqrt{v \varepsilon}} + C_{1\varepsilon} \frac{\varepsilon}{k} C_{3\varepsilon} G_b + S_\varepsilon \quad (9)$$

where

$$C_1 = \max \left[0.43, \frac{\eta}{\eta + 5} \right], \eta = S \frac{k}{\varepsilon}, S = \sqrt{2 S_{ij} S_{ij}} \quad (10)$$

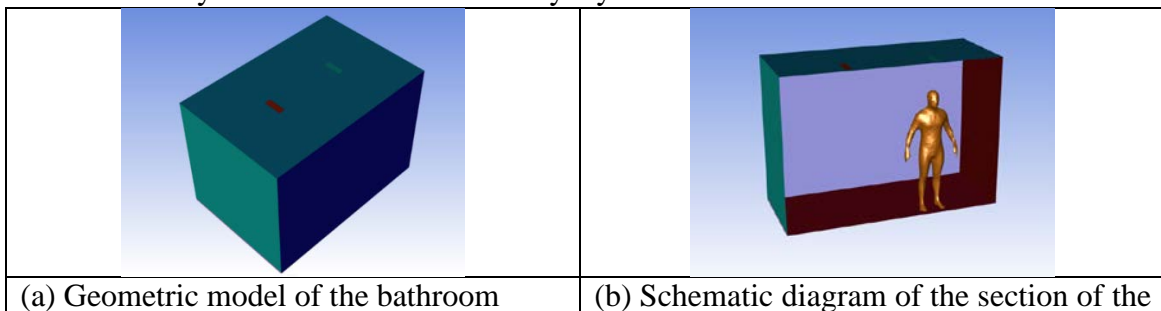
where G_K and G_b denote turbulent energy, G_K arises due to the presence of mean velocity gradient, G_b arises due to the presence of buoyancy; Y_M denotes the percentage of pulsation dispersion of compressible fluid in turbulent flow to the overall dissipation rate; C_2 , $C_{1\varepsilon}$ denote constants; σ_K , σ_ε denote the turbulent Prandtl number of K and ε ; and user-defined source terms are denoted by S_K , S_ε .

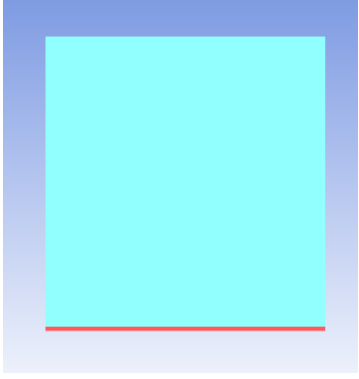
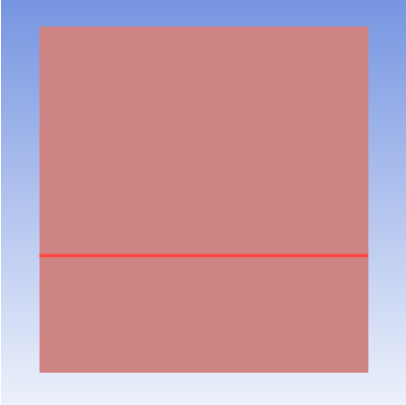
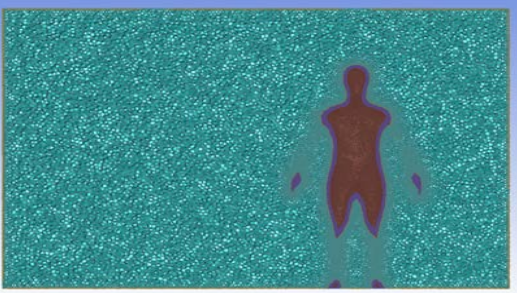
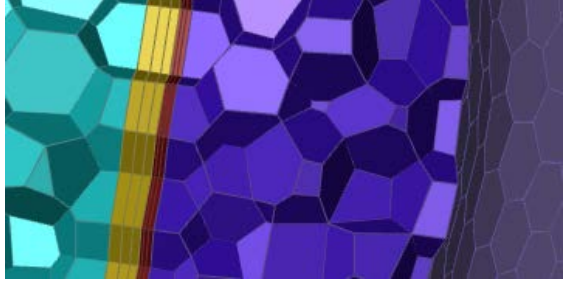
2.2 Geometry and Mesh

The geometric model used for this simulation is shown in Fig. 1(a), with dimensions of 3 m long, 2 m wide, and 2 m high. The two openings above are used to simulate two air inlets at different installation locations (inlet 1 on the left and inlet 2 on the right), with dimensions of 0.3 m long and 0.1 m wide. The mannequin is placed directly below inlet 2, and the schematic diagram is shown in Fig. 1(b).

In addition, in real life, the bathroom windows and doors usually have air leakage gaps, which will make this area become a pressure outlet, so the geometric model is simplified here. The left and right walls of the bathroom geometric model are drawn with 0.01m wide openings as pressure outlets, which are used to simulate the gaps in the bathroom doors and windows. The schematic diagrams are shown in Fig. 1(c) and Fig. 1(d);

The meshing of the bathroom geometry model and human body model is shown in Fig. 1(e), and the number of mesh is 2,266,012 and the number of nodes is 10,158,708. Among them, the local schematic of human body meshing is shown in Fig. 1(f). The red boundary layer and several blue layers are used to simulate the human surface skin, which is used as the computational domain for the heat transfer between air and skin surface and the heat conduction between skin surface and human tissues. The yellow mesh is the boundary layer for the air simulation.



bathroom geometry model	
	
(c) Pressure outlet on the left wall of the geometric model (red highlighted part)	(d) Pressure outlet on the right wall of the geometric model (red highlighted part)
	
(e) Bathroom geometry model and manikin meshing	(f) Local schematic diagram of human body meshing
Fig. 1 Geometric model and meshing of simulation experiment	

3. Results

This chapter presents the numerical simulation results of the effect of the different locations of the bathroom wind heaters installation on the human body during showering. It mainly analyzes the velocity field, pressure field and temperature field in the heat transfer process. From these three aspects, the heat exchange effect and thermal comfort of human body in two installation positions of bathroom wind heaters (inlet1 and inlet2) were compared. Moreover, during the simulation, the system was set to operate at variable power, i.e., four levels of wind heating power were used for comparison to increase the generalizability of the simulation results. The four power levels are 2,200w (high), 2,000w (medium), 1,800w (relatively low), and 1,600w (low). Based on heat transfer and engineering thermodynamics, the conversions to air temperature are 338K, 332K, 327K and 321K, respectively.

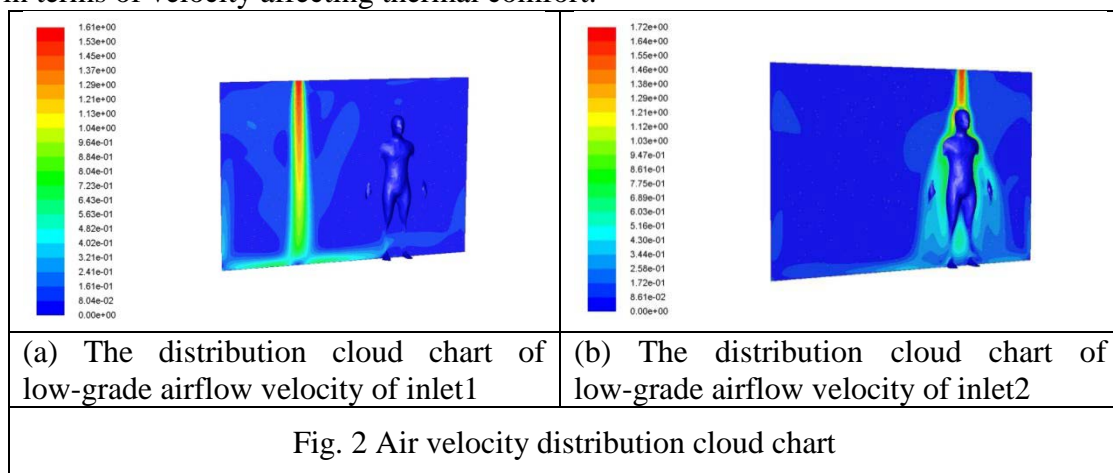
3.1 Velocity distributions

Fig. 2 show the velocity distribution clouds in the YZ plane of the geometric model, at X=0m and on the human skin surface. Since the air is assumed to be an incompressible fluid in the experiment, the air density does not change with temperature, and the inlet velocity is constant, the air velocity distribution is the same at the same inlet condition.

When the air inlet is inlet1, in Fig.2(a), for example, we can see that when the warm air is sent into the bathroom, its movement shows a jet state, and its jet range in the Z-axis direction has a slight trend to expand. In the Y-axis direction, because of the influence of buoyancy, the jet velocity gradually decreases. That is, the further away from the air inlet, the smaller the air flow velocity. When the hot air blows to the ground, it is blocked by the ground and spreads to the left and right sides respectively. In addition, because the inlet air velocity is small, its movement does not spread around the human body, and the air velocity distribution is more uniform in the shower area. The

velocity of air movement around the human body model is close to 0m/s, which does not produce the feeling of blowing wind and has a good comfort level[5].

When the air inlet is inlet2, in Fig. 2(b) for example, we can see that when the warm air is sent into the bathroom, its movement also shows the jet state, but because the human body is directly below it, its jet state is disturbed by the human body, and does not show the same jet law as inlet1 conditions. However, the two conditions have one thing in common that in the Y-axis direction, the further away from the air inlet, the smaller the air flow velocity. When the air blows to the head of the manikin, its movement also presents a small backflow. The air movement around the manikin is more violent and unevenly distributed, and its wind velocity is distributed between 0.516m/s~1.12m/s, which brings obvious wind sensation to the human body. The heating, ventilation and air conditioning design code stipulates that the indoor air velocity of thermal comfort air conditioners should not be greater than 0.2m/s in winter and 0.3m/s in summer. Therefore, when inlet2 is used as the air inlet, the air velocity will exceed the appropriate air velocity for comfort, and the thermal comfort effect of inlet2 as the air inlet is inferior to that of inlet1 in terms of velocity affecting thermal comfort.



3.2 Temperature distributions

In this paper, a brand of bathroom wind heaters was used as the object of study, and the heat transfer performance and indoor airflow organization were simulated during the operation of wind heating using FLUENT software[6]. The fluid flow and heat transfer characteristics of wind heating were analyzed. The internal structure of the bathroom and the human skin tissue were simplified in accordance with the normal human winter shower, and the effect of different installation positions of the wind heating on the movement of the indoor airflow and the heat transfer effect with the human body was studied[7]. The main conclusions are as follows:

(1) When inlet2 is used as the air inlet, the air velocity exceeds the appropriate air velocity for comfort. In terms of speed affecting thermal comfort, inlet2 is not as effective as inlet1 in terms of thermal comfort as air inlet.

(2) When inlet2 is the air inlet, the negative pressure in the bathroom may lead to the cold air from the left and right walls of the door and window gaps into the bathroom, resulting in the consumption of heat in the bathroom, affecting the heat exchange between indoor hot air and human body[8].

(3) When inlet1 and inlet2 are used as variables to compare indoor air temperature distribution and human skin surface temperature, inlet1 is used as air inlet to better meet indoor air quality standards and human thermal comfort.

4. Conclusion

From the above conclusions, it can be concluded that in the numerical simulation of the installation location of wind heating in the bathroom, the heat transfer effect is better with inlet1 as the air inlet due to its comparative working conditions. In other words, the installation of wind

heating at 100 cm away from the human shower position can provide a more comfortable shower experience and satisfy the human thermal comfort.

Acknowledgement

Youth Research Fund of Southeast University Chengxian College under Grant z0037

References

- [1] ASHRAE Standard 62-1999. Ventilation for Acceptable Indoor Air Quality.1999.
- [2] J.D.Spengter,J.M.Samet,J.F.Mc Carthy.Indoor Air Quality HandbooK.the 1st edition. NewYorK: Mc Graw-Hill Companies,Inc.2001.
- [3] P.VNielsen. Flow in air conditioned rooms(English Translation): [Ph D Thesis] Copenhagen: Technical University of Denmark, 1976.
- [4] E. Halawa,J. van Hoof. The adaptive approach to thermal comfort: A critical overview[J]. Energy & Buildings,2012,51.
- [5] Jingchun Min,Yicun Tang. Theoretical analysis of water film evaporation characteristics on an adiabatic solid wall[J]. International Journal of Refrigeration,2015,53.
- [6] ASHRAE fundamentals handbooK,[Chapter 8] 1993.
- [7] Gordon RG,Rober RB,Horvash SM.IEEE Trans 1976;BME-23:434-44.
- [8] Shuzo MuraKami,ShinsuKe Kato,Jie Zeng. Combined simulation of airflow, radiation and moisture transport for heat release from a human body[J]. Building and Environment,2000,35(6).